

JPET #245027

TITLE PAGE

A potent antagonist of protease-activated receptor 2 that inhibits multiple signaling functions in human cancer cells

Yuhong Jiang, Mei-Kwan Yau, Junxian Lim, Kai-Chen Wu, Weijun Xu, Jacky Y. Suen, David P. Fairlie*

Centre for Inflammation and Disease Research and Australian Research Council Centre of Excellence in Advanced Molecular Imaging, Institute for Molecular Bioscience, The University of Queensland, Brisbane, Qld, Australia (Y.J, M.K.Y, J.L, K.W, W.X, J.Y.S, D.P.F)

JPET #245027

RUNNING TITLE PAGE

Running Title: PAR2 antagonism in cancer cells

***Corresponding author:** Professor David P. Fairlie,

Centre for Inflammation and Disease Research and Australian Research Council Centre of Excellence in Advanced Molecular Imaging, Institute for Molecular Bioscience, The University of Queensland, Brisbane, Qld 4072, Australia

Telephone: +61733462989, Email: d.fairlie@imb.uq.edu.au.

Number of text pages: 30

Number of tables: 1

Number of figures: 7

Number of references: 55

Number of words in abstract: 248

Number of words in introduction: 749

Number of words in results: 1689

Number of words in discussion: 1498

A list of nonstandard abbreviations

CTGF, connective tissue growth factor; ERK, extracellular signal-regulated kinase; GPCRs, G-protein coupled receptors; GM-CSF, granulocyte macrophage colony-stimulating factor; HT-29, human colon adenocarcinoma grade II cell line; IL-6 interleukin-6; IL-8, interleukin-8; MDA-MB-231, human breast adenocarcinoma cells; PARs, protease-activated receptors; PAR2, protease-activated receptor 2; RhoA, Ras homologue gene family, member A.

JPET #245027

Recommended section assignment: Cellular and Molecular, Drug Discovery and Translational

Medicine, Other

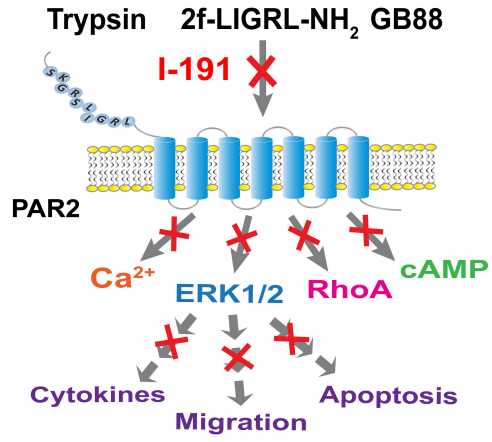
JPET #245027

ABSTRACT

Protease-activated receptor 2 (PAR2) is a cell surface protein linked to G-protein dependent and independent intracellular signaling pathways that produce a wide range of physiological responses, including those related to metabolism, inflammation, pain and cancer. Certain proteases, peptides and nonpeptides are known to potently activate PAR2. However, no effective potent PAR2 antagonists have been reported yet despite their anticipated therapeutic potential. This study investigates antagonism of key PAR2-dependent signaling properties and functions by an imidazopyridazine compound, I-191, in cancer cells. At nanomolar concentrations, I-191 inhibited PAR2 binding of, and activation by, structurally distinct PAR2 agonists (trypsin, peptide, nonpeptide) in a concentration-dependent manner in HT-29 cells. I-191 potently attenuated multiple PAR2-mediated intracellular signaling pathways leading to Ca^{2+} release, ERK1/2 phosphorylation, RhoA activation and inhibition of forskolin-induced cAMP accumulation. The mechanism of action of I-191 was investigated using binding and calcium mobilization studies in HT29 cells where I-191 was shown to be non-competitive and a negative allosteric modulator of the agonist 2f-LIGRL-NH₂. The compound alone did not activate these PAR2-mediated pathways, even at high micromolar concentrations, indicating no bias in these signaling properties. I-191 also potently inhibited PAR2-mediated downstream functional responses, including expression and secretion of inflammatory cytokines, cell apoptosis and migration, in human colon (HT-29) and breast (MDA-MB-231) cancer cells. These findings indicate that I-191 is a potent PAR2 antagonist that inhibits multiple PAR2-induced signaling pathways and functional responses. I-191 may be a valuable tool for characterising PAR2 functions in cancer and in other cellular, physiological and disease settings.

JPET #245027

VISUAL ABSTRACT



INTRODUCTION

Protease-activated receptors are unusual rhodopsin-like G-protein coupled receptors in being activated by proteases (e.g. trypsin, thrombin), which cleave within the extracellular N-terminus to expose an activating sequence (Arora *et al.*, 2007; Coughlin, 2000; Tuteja, 2009; Yau *et al.*, 2013). PAR2 is the most highly expressed PAR in certain immune and cancer cells. Upon activation, PAR2 mediates intracellular coupling to heterotrimeric G proteins that trigger pathway-dependent signaling (e.g. Ca²⁺ release, ERK1/2 phosphorylation, RhoA activation) as well as G protein-independent β -arrestin 1/2 signaling (Rothmeier and Ruf, 2012; Suen *et al.*, 2014). PAR2 signaling pathways are involved in circulatory, cardiovascular, central nervous, gastrointestinal, metabolic and respiratory systems (Ossovska and Bunnett, 2003; Lam and Schmidt, 2010; Rothmeier and Ruf, 2012; Saito and Bunnett, 2005). The consequent modulation by PAR2 of a wide range of physiological and disease processes in these tissues, including inflammation, cancer, respiratory and central nervous system dysfunction, highlights PAR2 as a potential unexploited therapeutic target (Knight *et al.*, 2001; Matej *et al.*, 2007; Reed *et al.*, 2003).

PAR2 is mainly activated by serine proteases (e.g. trypsin, tryptase, TF-FVII-FXa, matriptase) (Darmoul *et al.*, 2004; McLarty *et al.*, 2011; Mihara *et al.*, 2016; Ramachandran *et al.*, 2011; Seitz *et al.*, 2007), while some proteases cleave at a non-canonical site to produce a different activating sequence and different signaling profiles (Hollenberg *et al.*, 2014; Zhao *et al.*, 2015). Synthetic peptides also activate PAR2 (e.g. SLIGRL-NH₂, 2-furoyl-LIGRL-NH₂) (Barry *et al.*, 2010; Kawabata *et al.*, 2005; Yau *et al.*, 2015), some being biased agonists (e.g. 2f-LAAAI-NH₂, Isox-Cha-Chg-NH₂, Isox-Cha-Chg-Ala-Arg-NH₂) that signal more effectively through one pathway than another (Jiang *et al.*, 2017). The beneficial effects of PAR2 activation

JPET #245027

in vivo remain uncertain and context dependent, with pathway-selective biased ligands potentially being helpful in elucidating and harnessing therapeutic potential.

PAR2 antagonists might have disease-modifying properties but only a few weakly potent antagonists are known to test this possibility. ENMD-1068 weakly inhibits PAR2-mediated Ca^{2+} signaling *in vitro* (IC_{50} 5 mM) and joint inflammation *in vivo* (Kelso *et al.*, 2006), although it is uncertain if this was via PAR2. A more potent peptidic PAR2 antagonist (K-14585) inhibits p38 MAPK activation and IL-8 secretion, but promotes them above 10 μM concentrations (Goh *et al.*, 2009). GB83 and GB88 (IC_{50} 1–10 μM) and analogues inhibit PAR2 activation by proteases (e.g. trypsin, tryptase), peptides (e.g. SLIGRL-NH₂, 2-furoyl-LIGRLO-NH₂) and nonpeptides (e.g. GB110) as measured by Ca^{2+} release in multiple cell types (Barry *et al.*, 2010; Suen *et al.*, 2012; Yau *et al.*, 2016). However, while GB88 is an antagonist in inhibiting PAR2-induced calcium mobilization but an agonist in stimulating RhoA activation, promoting ERK1/2 phosphorylation, and reducing forskolin-stimulated cAMP (Suen *et al.*, 2014). A different peptidomimetic C391 is a weak PAR2 antagonist of Ca^{2+} (IC_{50} 1.3 μM) and pERK (IC_{50} 14 μM) signaling, as well as pain responses *in vivo* (Boitano *et al.*, 2015). Heptares and Astra-Zeneca reported an imidazole (AZ8838, IC_{50} 4.2 μM vs trypsin; 2.3 μM vs SLIGRL) and a benzimidazole (AZ3451, IC_{50} 6.6 μM vs trypsin; 5.4 nM vs SLIGRL) that bind at different sites in PAR2 crystal structures and inhibit Ca^{2+} (Cheng *et al.*, 2017). In summary, most PAR2 antagonists are active at only μM concentrations, do not inhibit all types of PAR2 agonists (proteases, peptides, nonpeptides), their activity can be context and cell dependent, or they have only been reported to date to be capable of inhibiting Ca^{2+} signaling (Yau *et al.*, 2016).

A diverse series of imidazopyridazine derivatives was recently claimed in a patent to antagonize PAR2-induced intracellular Ca^{2+} release at μM -nM concentrations (Farmer *et al.*,

JPET #245027

2015), although there was no evidence supporting selective binding to PAR2. Here we show that one imidazopyridazine derivative (I-191) displaces the binding of a fluorescent agonist from PAR2, and inhibits multiple PAR2-mediated signaling pathways and related functions in colorectal and breast carcinoma cells. I-191 is a full antagonist, with no agonist activity alone, of both trypsin- and peptide- (2f-LIGRL-NH₂) induced Ca²⁺ release, ERK1/2 phosphorylation, RhoA activation and inhibition of forskolin-induced cAMP accumulation in HT-29 cells. Furthermore, I-191 also inhibits ERK1/2 phosphorylation, RhoA activation and inhibition of forskolin-stimulated cAMP accumulation induced by μM concentrations of biased ligand GB88. The antagonist function of I-191 is established here by: (1) inhibition of PAR2-induced expression of inflammatory genes and proteins that have been previously associated with PAR2 activation, (2) inhibition of PAR2-reduced apoptosis-related caspase cleavages, and (3) inhibition of PAR2-triggered migration of HT-29 or MDA-MB-231 cancer cells. These findings indicate that I-191 is a potentially valuable tool *in vitro* for probing roles of PAR2 in physiology.

JPET #245027

MATERIALS AND METHODS

Cell Culture. All cell culture reagents were purchased from Invitrogen (Carlsbad, CA, USA) and Sigma Aldrich (St. Louis, MO, USA). HT-29 and MDA-MB-231 cells were a gift from the Queensland Medical Research Institute (Brisbane, Australia). HT-29 cells were maintained in DMEM at 37°C and 5% CO₂ while MDA-MB-231 cells were cultured in Leibovitz's L15 medium at 37°C without CO₂. All media were supplemented with 10% FBS, 100 units/mL penicillin and 100 units/mL streptomycin.

Binding assay. Assays were performed as previously described (Hoffman *et al.*, 2012; Suen *et al.*, 2014). Cells were seeded overnight in a 384-well plate at 2.4×10^4 cells/well, followed by PBS with 2% BSA blocking for 1 h at 37° C. Cells were simultaneously exposed to 2f-LIGRLO (diethylenetriaminepentaacetate-europium)-NH₂ (300 nM) and PAR2 ligands for 30 min. Cells were washed by PBS mixed with 20 μM EDTA, 0.01% Tween and 0.2% BSA. Cells were finally incubated with DELFIA enhancement solution (Perkin Elmer) for 90 min. Fluorescence was measured using a Pherastar FS fluorimeter (BMG, Germany).

Intracellular calcium mobilization. Cells were seeded overnight in 96-well plates at 5×10^4 cells/well and then incubated in dye loading buffer (HBSS with 4 μM Fluo-3, 0.04% pluronic acid, 1% FBS and 2.5 mM probenecid) for 1 h at 37 °C. Cells were washed with HBSS before adding antagonists for 30 min. Plates were transferred to a FLIPR Tetra instrument (Molecular Device, CA, USA). PAR2 agonists were added 10 s after reading commenced and calcium signals were measured in real time (excitation at 480 nm and emission at 520 nm). Receptor residence time was determined by washout experiments. Antagonists were pre-incubated with cells for 30 min at 37 °C and then unbound antagonists were removed by washing with HBSS buffer. At every indicated time point, plates were read after agonist addition. 2f-

JPET #245027

LIGRL-NH₂ alone (5 μM) was used to measure maximum fluorescence due to Ca²⁺ sequestration by Fluo-3, with individual results normalized accordingly.

Agonist concentration-response curves with increasing concentration of antagonists were fitted to an operational model of allosterism (Gregory *et al.*, 2012; Kenakin, 2013).

$$Effect = \frac{E_m[\tau_A[A](K_B + \alpha\beta[B] + \tau_B[B]K_A)]^n}{([A]K_B + K_AK_B + K_A[B] + \alpha[A][B])^n + [\tau_A[A](K_B + \alpha\beta[B]) + \tau_B[B]K_A]^n}$$

E_m is the maximum possible response, $[A]$ is the molar concentration of agonist 2f-LIGRL-NH₂, K_A is the equilibrium dissociation constant of agonist 2f-LIGRL-NH₂. $[B]$ is the molar concentration and K_B is the equilibrium dissociation constant for the allosteric modulator. The cooperativity factor α is related to the affinity of agonist, while β represents efficacy of agonist. τ_A and τ_B represent the capacity of agonist and allosteric modulator to regulate receptor activation, respectively. Since I-191 showed no agonist activity, $\tau_B = 0$ and the formula simplified to:

$$Effect = \frac{E_m[\tau_A[A](K_B + \alpha\beta[B])]^n}{([A]K_B + K_AK_B + K_A[B] + \alpha[A][B])^n + [\tau_A[A](K_B + \alpha\beta[B])]^n}$$

Parameters that were held constant for I-191: $K_A = 10^{-7}$, $K_B = 10^{-8}$, $\tau_A = 10$, $E_m = 100$.

AlphaLISA Surefire pERK1/2 assay. Cells were seeded overnight in 384-well microplates at 2×10^3 cells/well and then serum-starved for 2 h at 37 °C, prior to treatment with PAR2 ligands dissolved in serum-free medium. Antagonists were pre-incubated for 10 min followed by stimulation with agonist for 10 min. Supernatant was removed and cell lysis buffer was added with shaking for 30 min at room temperature, followed by adding reaction mixture for 2 h. Phosphorylation of ERK1/2 was measured according to manufacturer's instructions (PerkinElmer, MA, USA) and read using a Pherastar FS fluorimeter (BMG Labtech).

JPET #245027

G-LISA RhoA Activation. Cells were seeded at 2×10^5 cells/well and serum-starved for 2 days. After treating with a PAR2 agonist for 20 min at 37°C, cells were lysed for RhoA detection. An antagonist was added to cells 1 h prior to the agonist. RhoA activation was measured using a G-LISA Biochem kit according to manufacturer's instructions (Cytoskeleton Inc., Denver, CO, USA). Briefly, cell lysates were added to the binding buffer and incubated at 4°C for 30 min. Antigen-presenting buffer was then added for 2 min after washing. Cells were incubated with anti-RhoA primary antibody for 45 min, and subsequently incubated with secondary antibodies for 45 min. The mixed HRP detection reagent was added for 15 min, then stopped with buffer before signal was read by measuring absorbance at 490 nm using a microplate spectrophotometer (Suen *et al.*, 2014).

cAMP accumulation assay. Cells were seeded overnight in 384-well proxiplates at 2.4×10^3 cells/well. Antagonists were pre-incubated for 10 min, followed by stimulation with agonist for 30 min, prior to treatment with PAR2 agonists and forskolin for 30 min at room temperature, then followed by adding cAMP detection reagent for 1 h at room temperature. cAMP accumulation was measured according to manufacturer's instructions (PerkinElmer, MA, USA) and read using a Pherastar FS fluorimeter (BMG Labtech).

Cytokine-induced cleavage of caspases 3 and 8. As previously described (Iablokov *et al.*, 2014), cells were seeded overnight at 5×10^5 cells per well. After serum starving for 1 h, cells were incubated for 30 min with different concentrations of a PAR2 antagonist, before addition of a PAR2 agonist. Caspase 3/8 cleavage was then induced through addition of IFN- γ (40 ng.mL⁻¹) for 5 min before adding TNF (10 ng.mL⁻¹) and incubated for a further 6 h.

Immunoblot. After treatment, cell lysates were prepared using lysis buffer supplemented with a protease and phosphatase inhibitor cocktail (Cell Signaling Tech, MA, USA). Cell lysates

JPET #245027

was separated by electrophoresis in a Blot Bistris Plus 4–12% gel, followed by electrical transfer using iBlot 2 Dry Blotting System. Membranes were incubated with primary antibodies and secondary antibodies (cleaved caspase 3, Cell Signaling Tech 9661; cleaved caspase 8, Cell Signaling Tech 9496; anti-rabbit antibody conjugated to HRP, Cell Signaling Tech) using the iBind™ Western System (Life Technologies, Camarillo, CA, USA) according to instructions. Exposure times were varied to eliminate signal saturation. GAPDH (Sigma Aldrich) was used as a loading control and band intensity was calculated with Image J.

RT-PCR. Cells were seeded overnight at a density of 5×10^5 cells per well in 12-well plates. Cells were serum-starved overnight, then pre-incubated with different antagonist concentrations for 30 min before adding a PAR2 agonist for 1 h. Cells were then lysed and RNA was isolated using ISOLATE II RNA Mini Kit (Bioline). Total RNA was extracted from cells, random oligo dT were initially incubated at 70°C for 10 min, and then cooled on ice for at least 1 min before being reverse transcribed with Superscript III (Invitrogen) at 50 °C for 50 min then at 70 °C for 10 min. Quantitative real time PCR was performed using a ViiATM 7 Real-Time PCR System (Life Technologies), cDNA, SYBER Green master mix (Life Technologies; Carlsbad, CA, USA) and primers. Genes were amplified for 40 cycles. Relative-gene expression was normalised against HPRT1 (Forward, TCAGGCAGTATAATCCAAAGATGGT; Reverse, AGTCTGGCTTATATCCAAC ACTTCG).

ELISA. Cells were seeded overnight at a density of 5×10^5 cells/well in 12-well plates. Cells were serum-starved overnight before exposing to various concentrations of an antagonist for 30 min. Cells were then treated with a PAR2 agonist for 24 h. Cell supernatants were collected and cytokine secretion was measured using an ELISA for human IL-8, according to manufacturer's instructions (BD Bioscience, CA, USA).

JPET #245027

Cell migration *in vitro*. HT-29 cells were seeded overnight at a density of 2×10^5 cells/well in 12 well plates. As described previously²⁶, after cells formed a confluent monolayer, a scratch gap was created using a p200 pipette tip. Cells were washed, to remove floating cells, and incubated with or without PAR2 agonists in serum-free medium. Antagonists were added for 30 min. before scratching the monolayer. The images of the scratch gap were acquired (at 0, 24 and 48 h) using a Nikon Ti-U inverted brightfield microscope. The scratch gap size was calculated using ImageJ. Scratch gap size was measured as the gap area at 48 h divided by the initial gap area at 0 h.

Transwell chemotaxis assay. The transwell system (polycarbonate filter insert with 8 μm pore size membrane, Corning Inc., NY, USA) was used to investigate cell migration. Both sides of the membrane were coated with collagen I and air dried for 2 minutes. Cells were dissociated using non-enzymatic cell dissociation solution and re-suspended in serum-free L-15 with 0.1% BSA. Cells were seeded (2.5×10^5 /insert) and allowed to incubate for 3h at 37°C. PAR2 ligands were diluted in serum-free L-15 with 0.1% BSA and added to the bottom chamber to stimulate cell migration. Antagonists were pre-incubated for 30 min in the upper chamber prior to agonist addition. The transwell plates were incubated at 37°C and cells allowed to migrate for 24 h. After incubation, cells in the top chamber of the membrane were removed carefully using a cotton swab and fixed in 4% PFA. The membrane was washed twice with PBS and stained with DAPI. Migrated cells on the underside of the membrane were counted using a Nikon Ti-U inverted brightfield microscope.

Statistical analysis. GraphPad Prism 7.0 was used to analyze all data (San Diego, CA). Statistical significance of differences between groups was measured using one-way ANOVA,

JPET #245027

followed by Dunnett's multiple comparisons test or Student's t-test. Data are presented as means of entire data set \pm SEM.

Materials. Bovine trypsin was purchased from Sigma (Cat. No. T1426). I-191 (4-(8-(*tert*-butyl)-6-(4-fluorophenyl)imidazo[1,2-*b*]pyridazine-2-carbonyl)-3,3-dimethylpiperazin-2-one) was synthesized and characterized as described in the Supporting Information. PAR2 activating peptide agonist 2f-LIGRL-NH₂ and an Eu-tagged ornithine-containing peptide 2f-LIGRLO(diethylenetriaminepentaacetate-europium)-NH₂ were synthesized in house as described (Suen *et al.*, 2012, Suen *et al.*, 2014).

RESULTS

Inhibition of PAR2 specific binding in HT-29 cells.

The compound I-191 (**Figure 1A**) is among a series of imidazopyridazine compounds recently described in a patent application by Vertex (Farmer *et al.*, 2015). Here we investigate PAR2 binding, signaling and functional properties for I-191 in HT-29 human colon adenocarcinoma cells, which express higher levels of PAR2 than other PARs (**Figure 1B**). A fluorescent analogue of the well-established PAR2 agonist peptide 2f-LIGRLO-NH₂ (Suen *et al.*, 2014), labelled on the ornithine sidechain with europium diethylenetriaminepentaacetate, was used in competitive binding experiments to assess specific ligand binding to PAR2. The unlabelled 2f-LIGRL-NH₂ was able to compete with the Eu-tagged peptide analogue for binding to HT-29 cells (**Figure 1C**) in a concentration-dependent manner (pIC₅₀ 6.4 ± 0.2). I-191 similarly displaced the Eu-tagged peptide for binding to HT-29 cells (**Figure 1C**) in a concentration-dependent manner (pIC₅₀ 7.1 ± 0.2), consistent with specific binding of I-191 to PAR2 on HT-29 cells. However, unlike 2f-LIGRL-NH₂, even the highest concentrations of the antagonist I-191 did not fully displace the binding of Eu-tagged 2f-LIGLRLO-NH₂ (~25% remaining) from HT29 cells. The binding study is consistent with an insurmountable mechanism.

To investigate whether the mechanism of binding of I-191 to PAR2 was competitive or non-competitive with peptide agonist, we measured the binding affinity of varying concentrations of 2f-LIGRL-NH₂ in the presence of Eu-tagged 2f-LIGRLO-NH₂ (300 nM) and with increasing concentrations of I-191 (**Figure 1D**). There was no significant rightward shift in the plots and the IC₅₀ for 2f-LIGRL-NH₂ was almost invariant in the presence of increasing concentrations of I-191 (30 nM – 3 μM). At the highest concentrations of I-191 (10, 30 μM), the

JPET #245027

agonist peptide was not completely displaced (only 75%) from the cells. This indicates that I-191 is non-competitive with 2f-LIGRL-NH₂ in binding to PAR2 on HT-29 cells.

Inhibition of PAR2-mediated Ca²⁺ release in HT-29 cells.

Next, we studied I-191 for inhibition of PAR2-induced calcium signaling. I-191 was a potent antagonist in inhibiting intracellular Ca²⁺ release induced by either 2f-LIGRL-NH₂ (pIC₅₀ 7.2 ± 0.1) or bovine trypsin (pIC₅₀ 6.7 ± 0.1) in HT-29 cells (**Figure 2A**). I-191 was an order of magnitude more potent than our previously reported antagonist GB88 under the same conditions (**Figure 2B**, **Table 1**). I-191 did not induce any agonist-induced calcium response at concentrations up to 100 μM (**Figure 2A**) and it was about 100 fold more selective for PAR2 than PAR1 in PC3 cells (**Supplemental Figure 1**) and HT29 cells (Farmer *et al.*, 2015). The duration of inhibition, reflecting receptor residence time, was determined through washout experiments using the calcium assay (**Figure 2C**, **2D**). After 1 h incubation, I-191 (1 μM) inhibited more than 50% of the intracellular Ca²⁺ release induced by 2f-LIGRL-NH₂ (5 μM), and no antagonist activity was observed after 3h. The corresponding receptor residence time half-life was 51 min for I-191 at 37 °C, compared with ~200 min for GB88 (20 μM). Thus, I-191 is a potent full antagonist of PAR2 in inhibiting Ca²⁺ release in HT-29 colon cancer cells.

The mechanism of PAR2 antagonism by I-191 was further investigated for the Ca²⁺ signaling pathway in HT-29 cells through inhibitory effects on PAR2-induced calcium mobilization, following pre-treatment of cells with escalating concentrations of I-191. The agonist-induced calcium response curve showed a rightwards shift, but a depression in the maximum response at the highest concentration of 2f-LIGRL-NH₂ supported a non-competitive and insurmountable mechanism of I-191 (**Figure 2E**). In addition, we measured the effect of I-

JPET #245027

191 on the Ca^{2+} response elicited by the native PAR2 agonist trypsin (**Figure 2F**). The inhibitory pattern for I-191 was similar against trypsin as for 2f-LIGRL-NH₂. Further, at 1 μM - 30 μM of I-191 against 2f-LIGRL-NH₂ (**Figure 2E**) or 2 μM -60 μM I-191 against trypsin (**Figure 2F**), no further antagonism of the Ca^{2+} response was obtained. This saturation effect is a hallmark of allosteric modulation. An allosteric modulator occupies its own binding site and, once the site is saturated, no further allosteric antagonist effect can be achieved (Kenakin, 2007; Kenakin *et al.*, 2006). Using an operational model of allosterism (Gregory *et al.*, 2012; Kenakin, 2013; Watterson *et al.*, 2017), we calculated the cooperativity for both affinity (α) and efficacy (β) of the “probe” 2f-LIGRL-NH₂ in the calcium response. The finding that $\alpha = 0.85 < 1.0$ and $\beta = 0.04 < 1.0$, suggests that I-191 may be a negative allosteric modulator of 2f-LIGRL-NH₂-induced PAR2 activation in Ca^{2+} mobilisation. This calculated binding cooperativity ($\alpha = 0.85$) is consistent with I-191 being non-competitive and insurmountable with the agonist probe 2f-LIGRL-NH₂. Together, the mechanistic data for binding and calcium release reveals that I-191 is a negative allosteric modulator that binds at a site on PAR2 that is distinct from 2f-LIGRL-NH₂.

Inhibition of other PAR2 signaling pathways in HT-29 cells.

I-191 was also an antagonist in attenuating ERK1/2 phosphorylation (**Figure 3A**) induced by either 5 μM 2f-LIGRL-NH₂ (pIC_{50} 7.8 ± 0.2) or 50 nM bovine trypsin (pIC_{50} 7.2 ± 0.2). In addition, the agonist effect of the biased ligand GB88, which on its own stimulates ERK1/2 phosphorylation, was inhibited by I-191 (pIC_{50} 7.4 ± 0.2). I-191 had greater antagonist activity in this ERK1/2 assay than in the calcium assay (5-fold greater against 2f-LIGRL-NH₂ and 3-fold against trypsin), suggesting it is a more potent ERK1/2 pathway inhibitor.

JPET #245027

Further, the PAR2 agonists 2f-LIGRL-NH₂, trypsin, and the calcium-biased PAR2 antagonist GB88, each significantly stimulated RhoA activation in HT-29 cells, with around a 3-fold increase compared to untreated cells (**Figure 3B**). This activation of RhoA was inhibited by pre-incubation of HT29 cells with I-191 (10 μM), highlighting I-191 as an antagonist of PAR2-mediated RhoA signaling.

I-191 was also found to stimulate an inhibition curve in PAR2 agonist-reduced forskolin-induced cAMP, under certain conditions where its concentration was below 10 μM, suggesting that it is an antagonist in another PAR2-dependent signaling pathway (**Figure 3C**).

To summarize, I-191 is the first antagonist reported to date to potentially inhibit all these signaling pathways in HT-29 cells.

Inhibition of PAR2-mediated cytokine production and PAR2-attenuated cytokine-induced cleavage of caspases in HT-29 cells.

In addition to examining the effect of I-191 on three different PAR2 signaling pathways above, we also aimed to study its effects on related functional responses in cancer cells. First, we investigated whether I-191 could inhibit gene expression and secretion of the inflammatory cytokine, IL-8, that has been associated with ERK1/2 signaling in HT-29 cells (Jiang *et al.*, 2017; Wang *et al.*, 2010). For gene expression (**Figure 4A**), 2f-LIGRL-NH₂ induced a 2.5-fold increase in *CXCL8* mRNA expression (IL-8) in HT-29 cells. I-191 (1 and 10 μM) decreased this expression to baseline, but lower concentrations had little effect. Similar results were observed for IL-8 protein secretion induced by 2f-LIGRL-NH₂, which was also inhibited by I-191 (IC₅₀ ~100 nM, **Figure 4B**).

JPET #245027

Although PAR2 agonists do not induce expression of certain cytokines like IFN- γ and TNF, they do inhibit caspase-3 and caspase-8 cleavage induced by a combination of IFN- γ and TNF. These caspase cleavages are hallmarks of cell apoptosis in HT-29 cells (Iablokov *et al.*, 2014), and we have previously linked PAR2 inhibition of these caspase cleavages to PAR2-dependent ERK1/2 signaling in HT-29 cells (Jiang *et al.*, 2017). Here, we studied the inhibitory effect of I-191 on this PAR2 attenuation of cytokine-triggered cleavage of caspase 3 (**Figure 4C**) and caspase 8 (**Figure 4D**). In the presence of 2f-LIGRL-NH₂, the IFN- γ /TNF combination failed to induce any caspase cleavages, but pre-treatment with I-191 (0.1, 1 or 10 μ M) resulted in caspase cleavages. Lower concentrations of I-191 (1, 10 nM) had no effect. These results for I-191 support the conclusion that PAR2 antagonism can inhibit cytokine production, as well as cytokine-related caspase cleavages, via ERK1/2 signaling in HT-29 colon cancer cells.

Inhibition of PAR2-activated migration of HT-29 cells.

Scratching of the surface of cell monolayers is a convenient and commonly used approach to measure the effects of compounds on cell migration, through monitoring the capacity of the cells over time to close the scratch gap (Liang *et al.*, 2007). This effect has also been used to screen for compounds that can promote wound healing. Recently we reported the effects of PAR2 agonists in promoting cell migration and linked this property to the ERK1/2 pathway (Jiang *et al.*, 2017). Here, we studied whether I-191 could inhibit PAR2-mediated migration of HT-29 cells into the scratch gap. In the absence of FBS, 2f-LIGRL-NH₂ narrowed the scratch gap size to ~60% after 24h and ~36% after 48h (**Figure 5**). On the other hand, I-191 showed a concentration-dependent inhibition of this narrowing, with 1 μ M and 10 μ M almost halting migration after 48h (~80%) compared to the effect of 2f-LIGRL-NH₂ alone (**Figure 5**). Even 100

nM I-191 could significantly reduce PAR2 stimulated cell migration after 48h (gap size ~56%) but there was no detectable effect at lower concentrations. Thus, I-191 potently attenuates PAR2 agonist-triggered migration of HT-29 cells, a property we have associated with inhibition of PAR2-mediated signaling through ERK1/2 phosphorylation.

Inhibition of PAR2-stimulated migration and cytokine expression in MDA-MB-231 breast cancer cells.

MDA-MB-231 breast cancer cells express PAR2 more highly than other PARs (**Figure 6A**). PAR2 is activated in MDA-MB-231 cells by the agonists, 2f-LIGRL-NH₂ or trypsin (Ge *et al.*, 2004b; Matej *et al.*, 2007) and this is inhibited by I-191 (**Supplemental Figure 2**). Therefore, I-191 was examined in transwell chambers to create two separate compartments for detecting PAR2-stimulated cell migration (chemotaxis). 2f-LIGRL-NH₂ (100 nM) stimulated ~3-fold cell migration of MDA-MB-231 cells (**Figure 6B**). The biased antagonist GB88 (3 μM, 10 μM) that only inhibits the Gq-Ca²⁺-PKC signaling pathway (Suen *et al.*, 2014) did not inhibit PAR2-mediated migration nor was it an agonist alone in inducing migration (**Supplemental Figure 3**). In contrast, pre-treatment with I-191 (1 μM) led to inhibition of the migration of MDA-MB-231 cells induced by 2f-LIGRL-NH₂ (**Figure 6B**).

Further, four important signaling proteins that regulate physiological responses were used to probe the effect of I-191 (**Figure 6C-F**). 2f-LIGRL-NH₂ significantly enhances gene expression of IL-6 (*IL6*, ~25-fold increase), IL-8 (*CXCL8*, ~90-fold increase), CTGF (*CTGF*, ~6-fold increase) and GM-CSF (*CSF2*, ~14-fold increase) in MDA-MB-231 cells. I-191 (10 μM or 1 μM) significantly inhibited the expression of all four cytokine genes induced by 2f-LIGRL-NH₂. These data for breast cancer cells are consistent with findings above for colorectal

JPET #245027

carcinoma cells, supporting I-191 as an inhibitor of PAR2-induced chemotaxis and cytokine production in MDA-MB-231 breast cancer cells.

DISCUSSION

G protein-coupled receptors play pivotal roles in cellular sensing and intracellular responses to extracellular ligands (Marinissen and Gutkind, 2001). About 30% of all pharmaceuticals target GPCRs and were developed to either turn their functions on or off. However, each membrane-spanning GPCR protein is linked to multiple G-protein dependent and independent signaling pathways, in turn linked to different physiological functions. Thus, although switching a GPCR on or off was once thought to activate all or none of the associated signaling pathways and functional responses linked to that GPCR, we now know that some ligands exhibit biased signaling and activate or inhibit only one or a subset of these pathways and functions. Biased signaling was originally thought to involve either G protein coupling or beta arrestin signaling, but it is now known to apply to differential modulation of all individual pathways linked to a GPCR (Hollenberg *et al.*, 2014; Suen *et al.*, 2014; Rankovic *et al.*, 2016). It is therefore conceivable that ligands can be developed to modulate one or a few signaling pathways linked to a GPCR without affecting other pathways, or at least without similarly affecting all other signaling and functional responses. Indeed, antagonists may even be more beneficial if they only inhibited a single GPCR-linked pathway associated with a disease, without inhibiting other pathways linked to the same GPCR but responsible for beneficial functional responses in the cell.

In the context of PAR2, it would be useful to have antagonists that can block all PAR2-mediated signal transduction, as well as antagonists that block just one or a few downstream

JPET #245027

signaling pathways (Suen *et al.*, 2014). They could be helpful molecular tools for teasing out the relative merits of complete versus selective blockade of individual PAR2-linked signaling pathways in cells. In disease settings like cancer, where PAR2 is highly expressed it may be more desirable to inhibit multiple PAR2-dependent signaling associated with metastasis, proliferation, angiogenesis, and other functions promoting tumour development (Chanakira *et al.*, 2017; Chang *et al.*, 2013; Dorsam and Gutkind, 2007; Xie *et al.*, 2015), whereas in other settings it may be more desirable to dampen some signaling such as that leading to pro-inflammatory functions while still engaging signaling that leads to beneficial anti-inflammatory actions. To date, no antagonists have been found to potently inhibit all types of PAR2 agonists (proteases, peptides, nonpeptide), nor has any antagonist been shown to potently inhibit all known signaling pathways and functions activated by PAR2. Here we investigated whether a new imidazopyridazine compound I-191 (Farmer *et al.*, 2015) binds to PAR2, acts as an antagonist of different agonists, the mechanism of antagonism, and whether it inhibits multiple PAR2 signaling functions or only blocks one or a subset of PAR2 signaling responses like GB88 (Suen *et al.*, 2014).

This study provides evidence that I-191 binds to PAR2, since it acts in a concentration-dependent manner to displace a PAR2 ligand, fluorescence labeled 2f-LIGRLO-NH₂, for binding to PAR2 in HT-29 colon cancer cells. I-191 had a surprisingly short residence time on PAR2 (**Figure 2C**), but was still able to attenuate calcium release induced in HT-29 cells by either a proteolytic (trypsin) or peptidic (2f-LIGRL-NH₂) agonist of PAR2. The potency of I-191 was about ten-fold higher than antagonist GB88 under the same conditions (Table 1). Furthermore, I-191 showed no agonist activity even at high μ M concentrations. This capacity to antagonize both

JPET #245027

proteolytic and non-proteolytic agonists of PAR2, as well as not displaying agonist activity at high concentrations, is not shared by all reported antagonists of PAR2 (Yau et al, 2013).

The antagonist mechanism for I-191 was also investigated. I-191 inhibited the binding of Eu-tagged 2f-LIGRLO-NH₂ to PAR2 in a concentration-dependent manner, but it could not completely displace the agonist even at high concentrations. This non-competitive and insurmountable binding suggested that I-191 may be an allosteric modulator (Christopoulos, 2002). Increasing concentrations of I-191 in PAR2 agonist-induced calcium release revealed a saturation phenomenon, supporting allosteric binding of I-191 to PAR2. A characteristic of allosterism is cooperativity between orthosteric and allosteric ligands, known as “probe dependence” (Valant *et al.*, 2012). Allosteric modulators can use different mechanisms of inhibition against different agonists of GPCRs (Watterson *et al.*, 2017). However, for PARs it is difficult to characterize allosteric mechanisms since there is no exogenous orthosteric ligand. Instead it is the protease-cleaved N-terminus of the receptor itself that acts as the tethered orthosteric agonist. Therefore, the close surrogate 2f-LIGRL-NH₂ was used as agonist and the definition of orthosteric versus allosteric relates specifically to whether I-191 binds to the same or different site on PAR2 as 2f-LIGRL-NH₂. I-191 proved to be a negative allosteric modulator ($\alpha = 0.85 < 1.0$, $\beta = 0.04 < 1.0$) of 2f-LIGRL-NH₂ based on an operational model of allosterism (Gregory et al., 2012; Kenakin, 2013).

This mechanistic interpretation needs qualification. Firstly, the agonist is not the endogenous PAR2 agonist. Most synthetic agonists are analogues of the tethered sequence SLIGKV, such as SLIGRL-NH₂, 2f-LIGRL-NH₂, GB110, AY77. Structurally diverse PAR2 agonists may enhance our understanding of PAR2 activation mechanisms and permit better mechanistic descriptions of antagonist mechanisms. Secondly, Ca²⁺ mobilisation induced by 2f-

JPET #245027

LIGRL-NH₂ (or SLIGRL-NH₂) versus trypsin is differentially influenced by PAR2 mutagenesis (Suen *et al.*, 2017), suggesting that even synthetic peptide agonists might bind to a different site on PAR2 than the tethered ligand unmasked by trypsin. Our results indicate that I-191 is a negative allosteric modulator that may bind at a site on PAR2 that is different from that occupied by 2f-LIGRL-NH₂ or tethered agonist. Thirdly, allosteric behaviour is context dependent and these ligands may behave differently under different conditions, in other cell types and signalling pathways (Gao and Jacobson, 2017). The description here of allosteric modulation may be context and system dependent.

I-191 is also the first PAR2 antagonist reported to potently inhibit ERK1/2 phosphorylation, RhoA and cAMP activation induced by PAR2 agonists. Three different PAR2 agonists (trypsin, 2f-LIGRL-NH₂, GB88) were used to produce these reporters in HT-29 cells and to measure inhibition by I-191. I-191 is also the first antagonist reported to inhibit PAR2 activation of ERK1/2, RhoA and cAMP by the biased ligand GB88. It was a more potent antagonist than the recently reported C391 (IC₅₀ 14 μM, pERK1/2) (Boitano *et al.*, 2015). RhoA and cAMP signaling is mediated by PAR2 activation (Greenberg *et al.*, 2003; Sriwai *et al.*, 2013; Suen *et al.*, 2014), but no PAR2 antagonist has been reported to inhibit this pathway until now.

Finally, we demonstrate that I-191 antagonises different cellular functions stimulated by PAR2 agonists in colon and breast cancer cells. PAR2 activation is known to induce migration, cytokine release and apoptosis in HT-29 cells (Darmoul *et al.*, 2004; Iablokov *et al.*, 2014; Wang *et al.*, 2010). PAR2 agonists may therefore have some benefit in promoting cell survival in normal cells, whereas antagonists might promote apoptosis but inhibit cytokine release in, and migration of, cancer cells and prevent disease progression. I-191 was found here to affect three PAR2-initiated functions linked previously to ERK1/2 phosphorylation in HT-29 cells (Jiang *et*

JPET #245027

al., 2017). Consistent with I-191 being a potent PAR2 antagonist of ERK1/2 phosphorylation in HT-29 cells, I-191 was found to inhibit (a) PAR2 agonist-induced IL-8 gene expression and protein secretion, (b) PAR2 agonist-attenuation of IFN- γ /TNF-induced caspase 3/8 cleavages related to apoptosis, and (c) cell migration into a scratch gap in HT29 cell monolayers.

Breast cancer progression and metastasis is another consequence of PAR2 activation (Ge *et al.*, 2004a; Matej *et al.*, 2007; Parisis *et al.*, 2013). PAR2 is overexpressed in 72% of breast cancer tissues but only 21% of normal tissues. MDA-MB-231 cells overexpress PAR2 and migrate along a PAR2 agonist gradient (Su *et al.*, 2009). Inhibitory effects of I-191 on PAR2-induced migration of MDA-MB-231 breast cancer cells are consistent with observations for HT-29 colon cancer cells, indicating potent antagonist properties in different cancer cell lines. Unlike the biased ligand GB88, which does not inhibit ERK1/2 activation or PAR2-induced migration, I-191 strongly inhibited 2f-LIGRL-NH₂-induced migration of MDA-MB-231 cells. When MDA-MB-231 cells were pretreated with I-191, the latter antagonized 2f-LIGRL-NH₂ stimulated expression of cytokines (IL-6, IL-8, GM-CSF, CTGF). I-191 also inhibited PAR2-induced calcium release in normal human cells that highly express PAR2, such as HEK293 and HUVEC cells but was not cytotoxic (**Supplemental Figure S4**).

In conclusion, this study supports I-191 as a potent, unbiased and full antagonist of human PAR2 in cancer cell lines. It inhibited PAR2-induced signaling activated *in vitro* by three different types of PAR2 agonists (protease, peptide, nonpeptide). It is the first potent antagonist *in vitro* of PAR2-mediated intracellular signaling through different pathways in HT29 cells, namely Ca²⁺ mobilization, ERK1/2 phosphorylation, RhoA activation and forskolin-induced cAMP accumulation. These PAR2 antagonist properties are manifested in inhibition *in vitro* of known PAR2-activated functional responses, namely cytokine expression, apoptosis and cell

JPET #245027

migration in colorectal or breast cancer cells (**Figure 7**). This establishes I-191 as a potentially valuable new molecular tool for interrogating and better understanding the roles of PAR2 in physiology and disease settings, and this study could lay the groundwork for developing a new therapeutic agent for treating PAR2-mediated disease.

ACKNOWLEDGMENTS

We thank Professor Kum Kum Khanna and Dr Glenn Boyle (Queensland Institute of Medical Research, Brisbane, Australia) for MDA-MB-231 and HT-29 cells, respectively; and the Australian Cancer Research Foundation (ACRF) for a Cancer Biology Imaging Facility (Brisbane, Qld, Australia) enabling access to microscopes.

AUTHORSHIP CONTRIBUTIONS

Participated in research design: Jiang, Yau, Lim, Suen, Fairlie

Conducted experiments: Jiang, Yau, Lim, Wu

Contributed new reagents or analytic tools: Yau

Performed data analysis: Jiang, Xu, Yau, Lim, Wu, Fairlie

Wrote or contributed to the writing of the manuscript: Jiang, Yau, Lim, Wu, Xu, Suen, Fairlie

REFERENCES

- Arora P, Ricks TK, Trejo J (2007). Protease-activated receptor signalling, endocytic sorting and dysregulation in cancer. *J Cell Sci* 120: 921-928.
- Barry GD, Suen JY, Le GT, Cotterell A, Reid RC, Fairlie DP (2010). Novel agonists and antagonists for human protease activated receptor 2. *J Med Chem* 53: 7428-7440.
- Boitano S, Hoffman J, Flynn AN, Asiedu MN, Tillu DV, Zhang Z, Sherwood CL, Rivas CM, DeFea KA, Vagner J, Price TJ (2015). The novel PAR2 ligand C391 blocks multiple PAR2 signalling pathways in vitro and in vivo. *Br J Pharmacol* 172: 4535-4545.
- Chanakira A, Westmark PR, Ong IM, Sheehan JP (2017). Tissue factor-factor VIIa complex triggers protease activated receptor 2-dependent growth factor release and migration in ovarian cancer. *Gynecol Oncol* 145: 167-175.
- Chang LH, Pan SL, Lai CY, Tsai AC, Teng CM (2013). Activated PAR-2 regulates pancreatic cancer progression through ILK/HIF α induced TGF α expression and MEK/VEGF-A-mediated angiogenesis. *Am J Pathol* 183: 566-575.
- Cheng RK, Fiez-Vandal C, Schlenker O, Edman K, Aggeler B, Brown DG, Brown GA, C Cooke RM, Dumelin CE, Doré AS, Geschwindner S, Grebner C, Hermansson NO, Jazayeri A, Johansson P, Leong L, Prihandoko R, Rappas M, Soutter H, Snijder A, Sundström L, Tehan B, Thornton P, Troast D, Wiggin G, Zhukov A, Marshall FH, Dekker N (2017). Structural insight into allosteric modulation of protease-activated receptor 2. *Nature* 545: 112-115.
- Christopoulos A (2002). Allosteric binding sites on cell-surface receptors: novel targets for drug discovery. *Nat Rev Drug Discov* 1: 198-210.
- Coughlin SR (2000). Thrombin signalling and protease-activated receptors. *Nature* 407: 258-264.
- Darmoul D, Gratio V, Devaud H, & Laburthe M (2004). Protease-activated receptor 2 in colon cancer trypsin-induced MAPK phosphorylation and cell proliferation are mediated by epidermal growth factor receptor transactivation. *J Biol Chem* 279: 20927-20934.
- Dorsam RT and Gutkind JS (2007). G-protein-coupled receptors and cancer. *Nat Rev Cancer* 7: 79-94.
- Farmer LJ, Fournier PA, Lessard S, Liu B, St-Onge M, Sturino C, Szychowski J, Yannopoulos C, Vallee F, Lacoste JE, Martel J, Bubenik M, Ramtohul Y, Sayegh C (2015). Imidazopyridazines useful as inhibitors of the PAR2 signaling pathway. Patent WO2015048245.

JPET #245027

Gao ZG and Jacobson KA (2017). Distinct signaling patterns of allosteric antagonism at the P2Y1 receptor. *Mol Pharmacol* 92: 613-626.

Ge L, Shenoy SK, Lefkowitz RJ, DeFea K (2004). Constitutive protease-activated receptor-2-mediated migration of MDA MB-231 breast cancer cells requires both beta-arrestin-1 and -2. *J Biol Chem* 279: 55419-55424.

Goh FG, Ng PY, Nilsson M, Kanke T, Plevin R (2009). Dual effect of the novel peptide antagonist K-14585 on proteinase-activated receptor-2-mediated signalling. *Br J Pharmacol* 158: 1695-1704.

Greenberg DL, Mize GJ, Takayama TK (2003). Protease-activated receptor mediated RhoA signaling and cytoskeletal reorganization in LNCaP cells. *Biochemistry* 42: 702-709.

Gregory KJ, Noetzel MJ, Rook JM, Vinson PN, Stauffer SR, Rodriguez AL, Emmitte YZ, Aspen CC, Andrew SF, Brian AC, Craig WL, Colleen MN, P. JC(2012). Investigating metabotropic glutamate receptor 5 allosteric modulator cooperativity, affinity, and agonism: enriching structure-function studies and structure-activity relationships. *Mol Pharmacol* 82: 860-875.

Hoffman J, Flynn AN, Tillu DV, Zhang Z, Patek R, Price TJ, Vagner J, Boitano S (2012). Lanthanide labeling of a potent protease activated receptor-2 agonist for time-resolved fluorescence analysis. *Bioconj Chem* 23: 2098-2104.

Iablokov V, Hirota CL, Peplowski MA, Ramachandran R, Mihara K, Hollenberg MD, MacNaughton WK(2014). Proteinase-activated receptor 2 (PAR2) decreases apoptosis in colonic epithelial cells. *J Biol Chem* 289: 34366-34377.

Jiang Y, Yau M-K, Kok WM, Lim J, Wu K-C, Liu L, *et al.* (2017). Biased signaling by agonists of protease activated receptor 2. *ACS Chem Biol* 12: 1217-1226.

Kawabata A, Oono Y, Yonezawa D, Hiramatsu K, Inoi N, Sekiguchi F, Honjo M, Hirofuchi M, Kanke T, Ishiwata H (2005). 2-Furoyl-LIGRL-NH₂, a potent agonist for proteinase-activated receptor-2, as a gastric mucosal cytoprotective agent in mice. *Br J Pharmacol* 144: 212-219.

Kelso EB, Lockhart JC, Hembrough T, Dunning L, Plevin R, Hollenberg MD, Sommerhoff CP, McLean JS, Ferrell WR (2006). Therapeutic promise of proteinase-activated receptor-2 antagonism in joint inflammation. *J Pharmacol Exp Ther* 316: 1017-1024.

Kenakin T (2007). Allosteric theory: taking therapeutic advantage of the malleable nature of GPCRs. *Curr Neuropharmacol* 5: 149-156.

Kenakin T (2013). Analytical pharmacology and allosterism: the importance of quantifying drug parameters in drug discovery. *Drug Discov Today: Technol* 10: e229-e235.

Kenakin T, Jenkinson S, Watson C (2006). Determining the potency and molecular mechanism of action of insurmountable antagonists. *J Pharmacol Exp Ther* 319: 710-723.

JPET #245027

Knight DA, Lim S, Scaffidi AK, Roche N, Chung KF, Stewart GA, Thompson PJ (2001). Protease-activated receptors in human airways: upregulation of PAR-2 in respiratory epithelium from patients with asthma. *J Allergy Clin Immunol* 108: 797-803.

Lam D and Schmidt B (2010). Serine proteases and protease-activated receptor 2-dependent allodynia: a novel cancer pain pathway. *Pain* 149: 263-272.

Liang C-C, Park AY, Guan J-L (2007). In vitro scratch assay: a convenient and inexpensive method for analysis of cell migration in vitro. *Nat Protocols* 2: 329-333.

M D Hollenberg KM, D Polley, J Y Suen, A Han, D P Fairlie, R Ramachandran (2014). Biased signalling and proteinase-activated receptors (PARs): targeting inflammatory disease. *Br J Pharmacol* 171: 1180–1194.

Marinissen MJ and Gutkind JS (2001). G-protein-coupled receptors and signaling networks: emerging paradigms. *Trends Pharmacol Sci* 22: 368-376.

Matej R, Mand akova P, Netikova I, Pouckova P, Olejár T (2007). Proteinase-activated receptor-2 expression in breast cancer and the role of trypsin on growth and metabolism of breast cancer cell line MDA MB-231. *Physiol Res* 56: 475.

McLarty JL, Meléndez GC, Brower GL, Janicki JS, Levick SP (2011). Trypsin/protease-activated receptor 2 interactions induce selective mitogen-activated protein kinase signaling and collagen synthesis by cardiac fibroblasts. *Hypertension* 58: 264-270.

Mihara K, Ramachandran R, Saifeddine M, Hansen KK, Renaux B, Polley D, *et al.* (2016). Thrombin-mediated direct activation of proteinase-activated receptor-2: Another target for thrombin signaling. *Mol Pharmacol* 89: 606-614.

Ossovskaya VS and Bunnett NW (2004). Protease-activated receptors- contribution to physiology and disease. *Physiol Rev* 84: 579-621.

Parisis N, Metodieva G, Metodiev MV (2013). Pseudopodial and β -arrestin-interacting proteomes from migrating breast cancer cells upon PAR2 activation. *J Proteomics* 80: 91-106.

Ramachandran R, Mihara K, Chung H, Renaux B, Lau CS, Muruve DA, *et al.* (2011). Neutrophil elastase acts as a biased agonist for proteinase-activated receptor-2 (PAR2). *J Biol Chem* 286: 24638-24648.

Rankovic Z, Brust TF, Bohn LM (2016). Biased agonism: An emerging paradigm in GPCR drug discovery. *Bioorg Med Chem Lett* 26: 241-250.

Reed DE, Barajas-Lopez C, Cottrell G, Velazquez-Rocha S, Dery O, Grady EF, *et al.* (2003). Mast cell tryptase and proteinase-activated receptor 2 induce hyperexcitability of guinea-pig submucosal neurons. *J Physiol* 547: 531-542.

Rothmeier AS and Ruf W Protease-activated receptor 2 signaling in inflammation. *Semin Immunopathol* 34 (1):133-149.

Saito T and Bunnett NW (2005). Protease-activated receptors. *Neuromolecular Med* 7: 79-99.

Seitz I, Hess S, Schulz H, Eckl R, Busch G, Montens HP, Brandl R, Seidl S, Shomig A, Ott I (2007). Membrane-type serine protease-1/matriptase induces interleukin-6 and-8 in endothelial cells by activation of protease-activated receptor-2. Potential implications in atherosclerosis. *Arterioscler Thromb Vasc Biol* 27: 769-775.

Sriwai W, Mahavadi S, Al-Shboul O, Grider JR, Murthy KS (2013). Distinctive G protein-dependent signaling by protease-activated receptor 2 (PAR2) in smooth muscle: feedback inhibition of RhoA by cAMP-independent PKA. *PloS One* 8: e66743.

Su S, Li Y, Luo Y, Sheng Y, Su Y, Padia R, Pan ZK, Dong Z, Huang S (2009). Proteinase-activated receptor 2 expression in breast cancer and its role in breast cancer cell migration. *Oncogene* 28: 3047-3057.

Suen J, Adams M, Lim J, Madala P, Xu W, Cotterell A, He Y, Yau M-K, Hooper JD, Fairlie DP (2017). Mapping transmembrane residues of proteinase activated receptor 2 (PAR2) that influence ligand-modulated calcium signaling. *Pharmacol Res* 117: 328-342.

Suen JY, Barry GD, Lohman RJ, Halili MA, Cotterell AJ, Le GT, Fairlie DP (2012). Modulating human proteinase activated receptor 2 with a novel antagonist (GB88) and agonist (GB110). *Br J Pharmacol* 165: 1413-1423.

Suen JY, Cotterell A, Lohman RJ, Lim J, Han A, Yau MK, Liu L, Cooper MA, Vesey DA, Fairlie DP (2014). Pathway-selective antagonism of proteinase activated receptor 2. *Br J Pharmacol* 171: 4112-4124.

Tuteja N (2009). Signaling through G protein coupled receptors. *Plant Signal Behav* 4: 942-947.

Valant C, Felder CC, Sexton PM, Christopoulos A (2012). Probe-dependence in the allosteric modulation of a G protein-coupled receptor: Implications for detection and validation of allosteric ligand effects. *Mol Pharmacol* 81:41-52

Wang H, Moreau F, Hirota CL, MacNaughton WK (2010). Proteinase-activated receptors induce interleukin-8 expression by intestinal epithelial cells through ERK/RSK90 activation and histone acetylation. *FASEB J* 24: 1971-1980.

Watterson KR, Hansen SV, Hudson BD, Alvarez-Curto E, Raihan SZ, Azevedo CM, Martin G, Dunlop J, Yarwood SJ, Ulven Tm Milligan G (2017). Probe-dependent negative allosteric modulators of the long-chain free fatty acid receptor FFA4. *Mol Pharmacol* 91: 630-641.

JPET #245027

Xie L, Duan Z, Liu C, Zheng Y, Zhou J (2015). Protease-activated receptor 2 agonist increases cell proliferation and invasion of human pancreatic cancer cells. *Exp Ther Med* 9: 239-244.

Yau M-K, Lim J, Liu L, Fairlie DP (2016) Protease activated receptor 2 (PAR2) modulators: a patent review (2010–2015). *Expert Opin Thera Patents* 26: 471-483.

Yau M-K, Liu L, Suen JY, Lim J, Lohman R-J, Jiang Y, Cotterell AJ, Barry GD, Mak JYW, Vesey DA, Reid RC, Fairlie DP (2016). PAR2 modulators derived from GB88. *ACS Med Chem Lett* 7: 1179-1184.

Yau M-K, Suen JY, Xu W, Lim J, Liu L, Adams MN, He YW, Hopper JD, Reid RC, David DP (2015). Potent small agonists of protease activated receptor 2. *ACS Med Chem Lett* 7:105-110.

Yau MK, Liu L, Fairlie DP (2013). Toward drugs for protease-activated receptor 2 (PAR2). *J Med Chem* 56: 7477-7497.

Zhao P, Lieu T, Barlow N, Sostegni S, Haerteis S, Korbmacher C, *et al.* (2015). Neutrophil elastase activates PAR2 and TRPV4 to cause inflammation and pain. *J Biol Chem* 290:13875-13887.

JPET #245027

FOOTNOTES

Unnumbered footnote providing the source of financial support:

This work was supported by the National Health and Medical Research Council for Senior Principal Research Fellowships (Grant 1027369, 1117017) and project grants (Grant 1084083, 1047759) and the Australian Research Council (Grant DP130100629, CE140100011) to D.P.F.

FIGURE LEGENDS

Figure 1. Specific binding of I-191 to PAR2 in HT-29 cells. (A) Structure of PAR2 ligand, I-191. (B). Relative human mRNA expression of PAR1-4 genes (*F2R*, *F2RL1*, *F2RL2*, *F2RL3*) in HT-29 cells, PAR2 having the highest expression. (C) Concentration-dependent binding with 300 nM Eu-labelled 2f-LIGRLO-NH₂ of 2f-LIGRL-NH₂ (pIC₅₀ 6.4 ± 0.2) or I-191 (pIC₅₀ 7.1 ± 0.2). 2f-LIGRLO-NH₂ and 2f-LIGRL-NH₂ are well-established PAR2-selective agonist ligands. (D). Concentration-dependent response of 2f-LIGRL-NH₂ in displacing 300 nM Eu-tagged 2f-LIGRLO-NH₂ binding to PAR2, in the presence of increasing concentrations of I-191 in HT-29 cells. Statistical analysis by one-way ANOVA followed by Dunnett's multiple comparisons test, each data point represents the mean ± SEM. *** p < 0.001 (n ≥ 3).

Figure 2. I-191 attenuates PAR2-induced Ca²⁺ signaling in HT-29 cells.

(A) I-191 attenuates Ca²⁺ induced in HT-29 cells by 5 μM 2f-LIGRL-NH₂ (pink) or 50 nM bovine trypsin (blue), but alone shows no agonist activity (black). (B) Known antagonist GB88 similarly attenuates Ca²⁺ in HT-29 cells but at ten-fold higher concentrations. (C, D) Duration of inhibition by (C) I-191 (1 μM) or (D) GB88 (20 μM) of Ca²⁺ release induced by 2f-LIGRL-NH₂ (5 μM) in HT-29 cells. (E) I-191 is a non-competitive and insurmountable antagonist inhibiting 2f-LIGRL-NH₂-induced Ca²⁺ release in HT-29 cells. The affinity parameter $\alpha = 0.85$ and efficacy parameter $\beta = 0.04$ indicate that I-191 is a negative allosteric modulator of the agonist 2f-LIGRL-NH₂. (F). I-191 is a non-competitive and insurmountable antagonist in blocking trypsin-induced Ca²⁺ release in HT-29 cells. Statistical analysis by one-way ANOVA followed by Dunnett's multiple comparisons test, each data point represents the mean ± SEM (n ≥ 3).

JPET #245027

Figure 3. I-191 inhibits PAR2-induced ERK1/2, RhoA and cAMP signaling in HT-29 cells.

(A). I-191 inhibits ERK1/2 phosphorylation induced in HT-29 cells by three PAR2 agonists, 2f-LIGRL-NH₂ (5 μM, pink), bovine trypsin (50 nM, blue) or biased ligand GB88 (10 μM, green), in a concentration-dependent manner. (B) I-191 (10 μM) inhibits RhoA activation induced in HT-29 cells by 2f-LIGRL-NH₂ (10 μM), bovine trypsin (10 nM) or GB88 (50 μM). (C). I-191 inhibits PAR2-reduced 100 nM forskolin-induced cAMP accumulation by 1 μM 2f-LIGRL-NH₂ (pink), 50 nM bovine trypsin (blue), or 5 μM GB88 (green) in a concentration-dependent manner, under conditions where the I-191 concentration was below 10 μM. Statistical analysis by one-way ANOVA followed by Dunnett's multiple comparisons test, each data point represents the mean ± SEM, * p < 0.05, ** p < 0.01 (n ≥ 3).

Figure 4. I-191 inhibits PAR2-induced cytokine gene expression, cytokine protein secretion, and PAR2-inhibited cytokine-induced caspase cleavages in HT-29 cells. (A-B).

Concentration-dependent inhibition by I-191 of (A) *CXCL8* gene expression and (B) IL-8 protein secretion induced by 2f-LIGRL-NH₂ (10 μM). (C-D). PAR2 agonist 2f-LIGRL-NH₂ (1 μM) blocks apoptosis induced by the combination of IFN-γ (40 ng. mL⁻¹) and TNF (10 ng. mL⁻¹) through inhibiting: (C) caspase 3 and (D) caspase 8 cleavages, whereas I-191 inhibits these effects in a concentration-dependent manner. Statistical analysis by one-way ANOVA followed by Dunnett's multiple comparisons test, *p < 0.05, **p < 0.01, *** p < 0.001 (n ≥ 3).

Figure 5. I-191 attenuates PAR2-induced migration of HT-29 cells in a concentration-dependent manner. (A) Concentration dependent inhibition by I-191 of cell migration induced by PAR2 agonist 2f-LIGRL-NH₂ (1 μM) into a scratch gap over 48 h. (B) Temporal effect on

JPET #245027

cell migration into a scratch gap over 48h by 2f-LIGRL-NH₂ (1 μM) alone and with varying concentrations of I-191 (1 nM, 10 nM, 100 nM, 1 μM, 10 μM). (C) Concentration-dependent inhibition by I-191 of cell migration over 48 h induced by PAR2 agonist 2f-LIGRL-NH₂ (1 μM) into a scratch gap. Statistical analysis by one-way ANOVA followed by Dunnett's multiple comparisons test, ** p < 0.01, *** p < 0.001 (n ≥ 3).

Figure 6. I-191 inhibits PAR2-induced migration and cytokine gene expression in MDA-MB-231 cells. (A) Cells expressed the PAR2 mRNA more highly than PAR1, PAR3 and PAR4. (B) Cell migration induced by PAR2 agonist 2f-LIGRL-NH₂ (100 nM) is inhibited by I-191 (1 μM). (C-F) 2f-LIGRL-NH₂ (1 μM) induces mRNA expression of (C) *IL6*, (D) *CXCL8*, (E) *CTGF* or (F) *CSF2*, which are inhibited by I-191 (1μM or 10 μM). Statistical analysis by one-way ANOVA followed by Dunnett's multiple comparisons test, * p < 0.05, ** p < 0.01, *** p < 0.001 (n ≥ 3).

Figure 7. Effect of I-191 (red cross) on intracellular signaling and cell functions induced by three different types of PAR2 agonist.

TABLES

Table 1. Comparative inhibition of PAR2-induced signals in HT-29 cells.

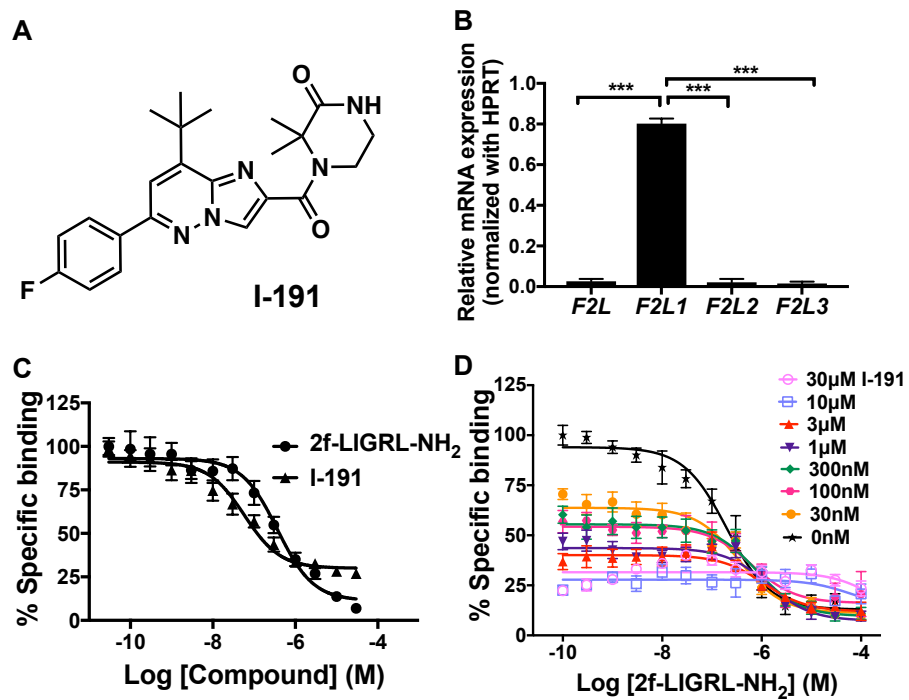
Compound (agonist)	iCa²⁺ (pIC₅₀ ± SEM)	pERK1/2 (pIC₅₀ ± SEM)	cAMP (pIC₅₀ ± SEM)	RhoA (pIC₅₀)
I-191 (2f-LIGRL-NH ₂) ^a	7.2 ± 0.1	7.8 ± 0.2	6.8 ± 0.3	~ 5.5 ^e
I-191 (Trypsin) ^b	6.7 ± 0.1	7.2 ± 0.2	6.6 ± 0.3	~ 5.5 ^e
I-191 (GB88) ^c	-	7.4 ± 0.2	6.5 ± 0.3	~ 5.5 ^e
GB88 (2f-LIGRL-NH ₂) ^d	6.0 ± 0.1	-	-	-
GB88 (Trypsin) ^d	5.7 ± 0.1	-	-	-

^aI-191 inhibits PAR2 signaling pathways activated by 2f-LIGRL-NH₂. ^bI-191 inhibits PAR2 signaling pathways activated by bovine trypsin. ^cI-191 inhibits PAR2 signaling pathways activated by GB88. ^dGB88 inhibits iCa²⁺ release induced by 2f-LIGRL-NH₂ or bovine trypsin. ^eEstimated from Figure 3B. n ≥ 3 for all data.

JPET #245027

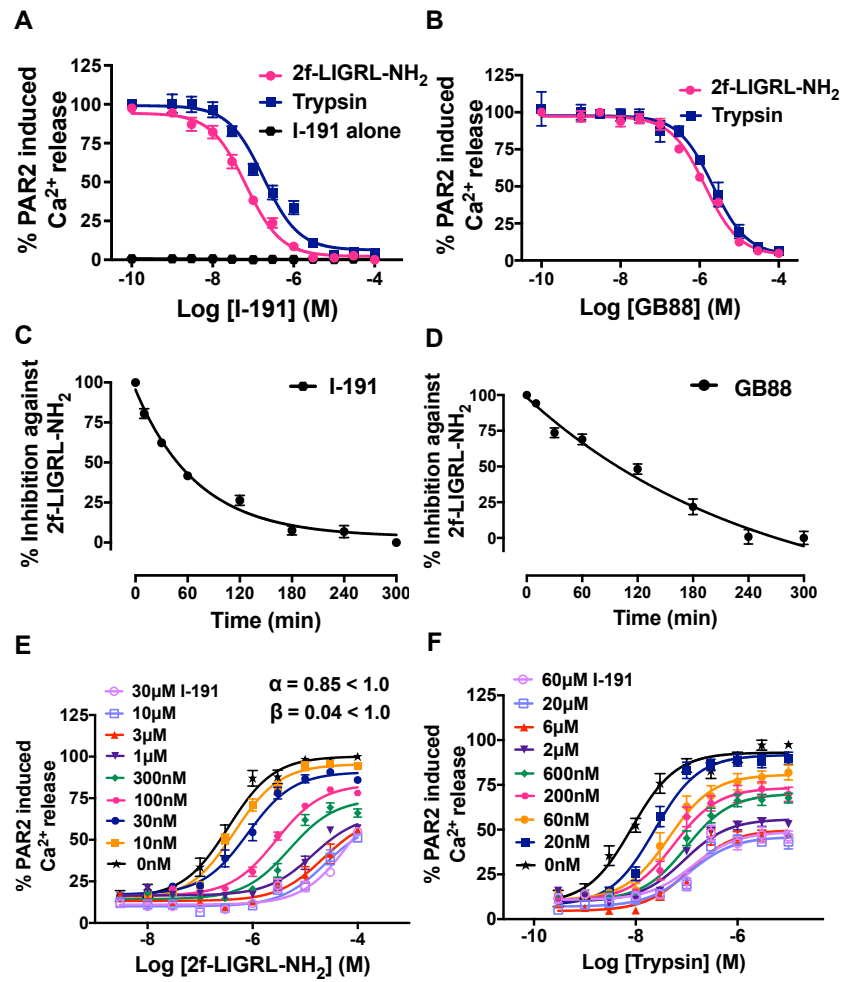
FIGURES

Figure 1



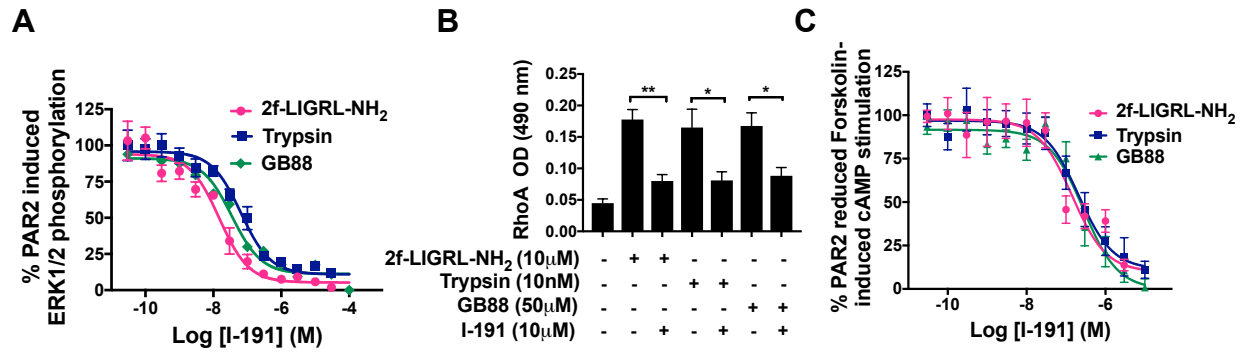
JPET #245027

Figure 2

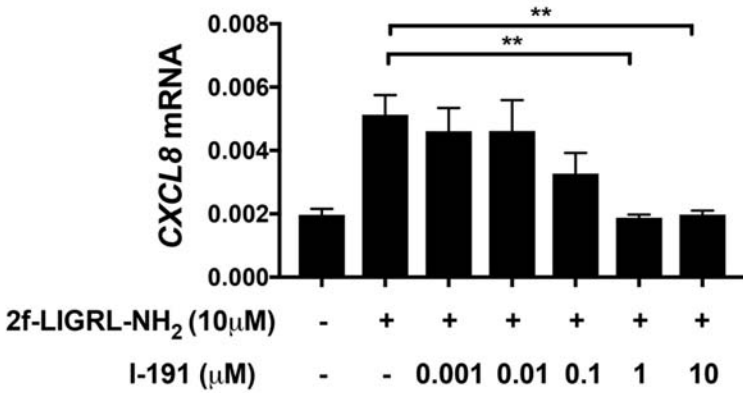


JPET #245027

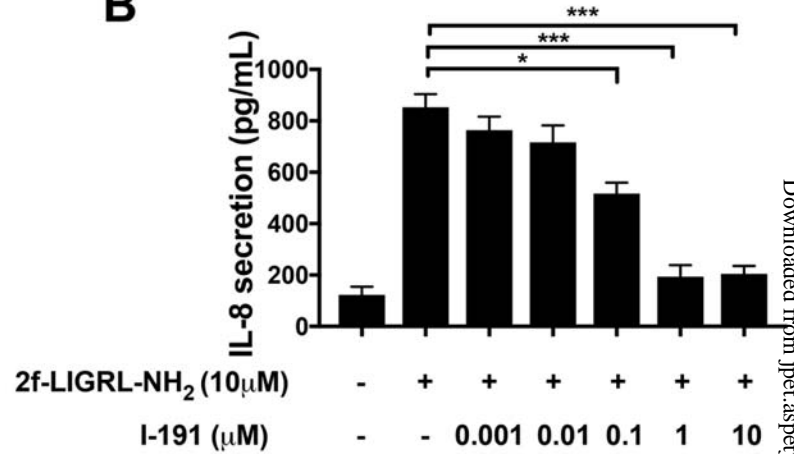
Figure 3



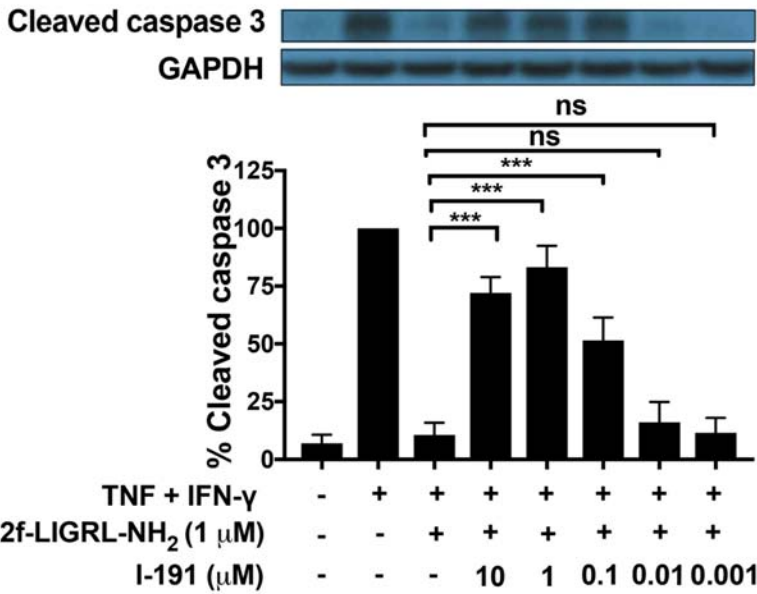
A



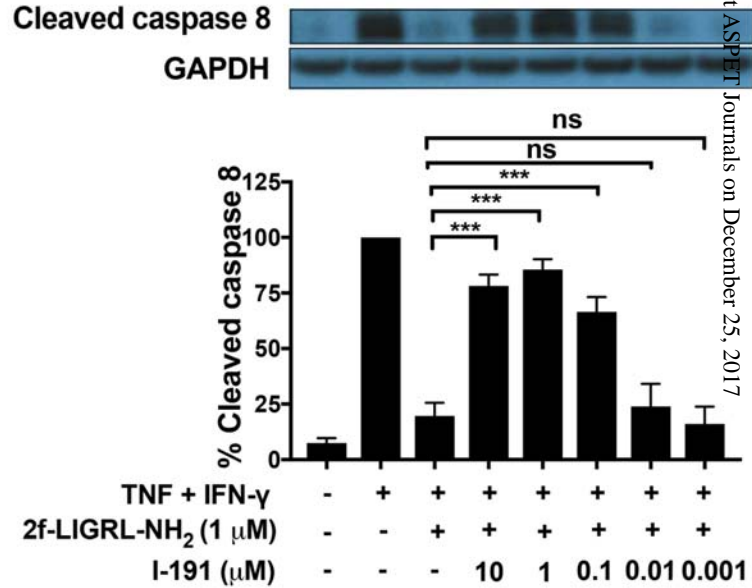
B



C

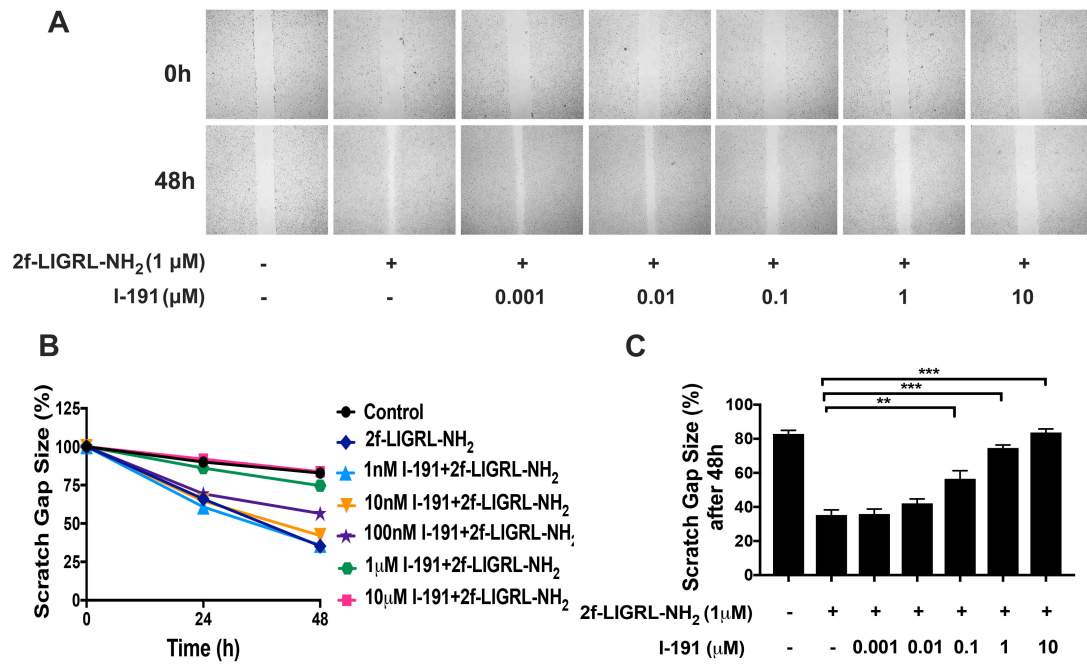


D



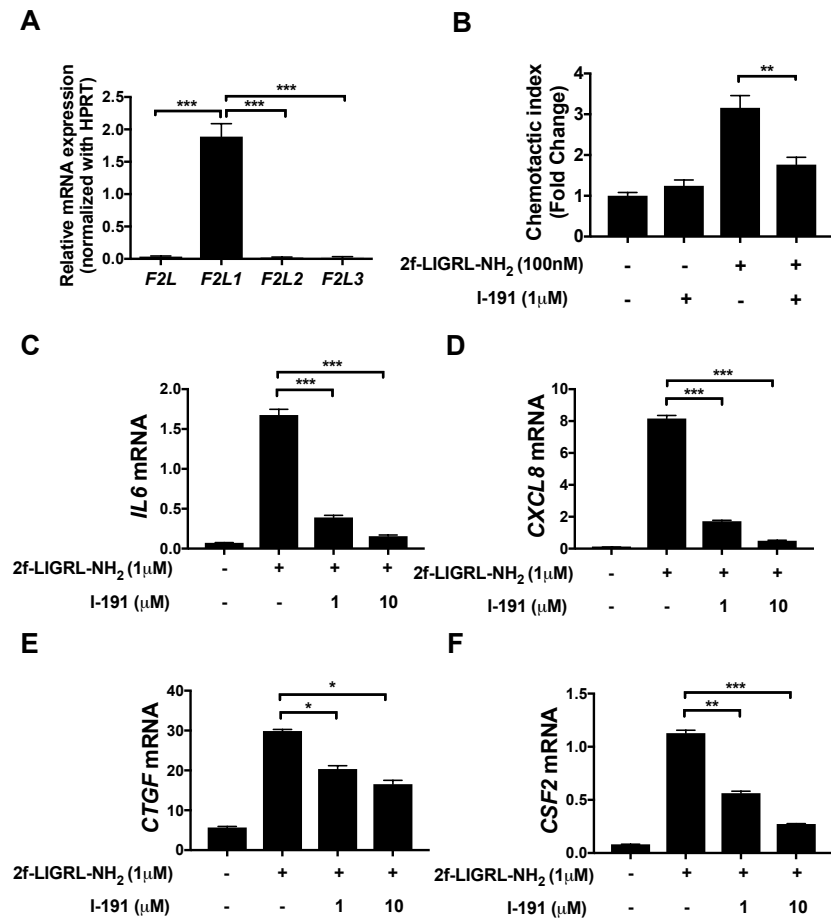
JPET #245027

Figure 5



JPET #245027

Figure 6



JPET #245027

Figure 7

